Hierarchical Sn-MFI zeolites prepared by facile top-down methods for sugar isomerisation

Author(s):
Dapsens, Pierre Y.; Mondelli, Cecilia; Jagielski, Jakub; Hauert, Roland; Pérez-Ramírez, Javier

Publication date:
2014-08-01

Permanent link:
https://doi.org/10.3929/ethz-a-010792732

Originally published in:
Catalysis Science & Technology 4(8), https://doi.org/10.1039/C4CY00172A

Funding acknowledgement:
140496 - Biomass to chemicals over tailored hierarchical zeolite-based catalysts (SNF)

Catalysis
Science & Technology

Dynamic Article Links ►

Cite this: DOI: 10.1039/c0xx00000x

www.rsc.org/xxxxxx

REPORT

Hierarchical Sn-MFI zeolites prepared by facile top-down methods for sugar isomerisation

Pierre Y. Dapsens,[a] Cecilia Mondelli,[a]* Jakub Jagielski,[a] Roland Hauert[b] and Javier Pérez-Ramírez[a]*

Received (in XXX, XXX) Xth XXXXXXXXX 20XX, Accepted Xth XXXXXXXXX 20XX
DOI: 10.1039/b000000x

Alkaline treatment of hydrothermally-synthesised Sn-MFI and alkaline-assisted stannation of silicalite-1 were investigated as industrially-amenable post-synthetic strategies to generate hierarchical Lewis-acidic MFI zeolites for the isomerisation of mono- and disaccharides. The mesoporosity introduced upon both treatments produced materials able to convert glucose, xylose, and lactose, which suffer from access or diffusion limitations to the active sites of the purely microporous Sn-MFI. The stannation of silicalite-1 rendered more active catalysts than the base leaching of Sn-MFI. This is due to the better utilisation of Sn, which is namely incorporated at the crystals' external surface in the former case but mostly remains in the inaccessible micropores in the latter. The amount of Sn introduced via stannation could also be controlled by varying the strength of the alkaline solution and the molarity of the tin salt added. A Sn loading of 0.25 wt.% already ensures remarkable activity and selectivity.

1 Introduction

In the last decade, metal-containing high-silica zeolites have gained significant interest as heterogeneous catalysts for the fossil fuel-based production of fine chemicals and for the transformation of renewable saccharide feedstocks into commodity chemicals.[1] In particular, Sn-BEA synthesised in fluoride media has shown outstanding performance in the liquid-phase aldo-ketose isomerisation of hexoses (*e.g.* glucose, galactose), pentoses (*e.g.* xylose, arabinose), and disaccharides (*e.g.* lactose) and in the H_2O_2-mediated Baeyer-Villiger oxidation of ketones (*e.g.* 2-adamantanone).[2] Its remarkable activity, selectivity, and stability originates from the presence of strong and isolated Lewis-acidic tin centres embedded in a crystalline and defects-free (*e.g.* Si-O^- or Si-OH) silica matrix.[3] The high hydrophobicity of the latter is believed to prevent extensive water diffusion into the microporous network, thus hindering irreversible deactivation by leaching of the active species. Still, the industrial viability of this catalyst is limited by the complexity of its synthesis, which requires (*i*) long aging times (40 days for the unseeded protocol) under precise stirring conditions to enable the complete incorporation of the metal into the framework [4] and (*ii*) stoichiometric amounts (relative to the structure-directing agent) of corrosive and noxious HF to ensure the minimisation of structural defects.[3a] Furthermore, as this method gives rise to large crystals, the long diffusion length is expected to lead to an underutilisation of the active zeolite microporous volume. This will be particularly emphasised in the processing of bulky substrates. Consequently, recent research efforts have focussed on the development of alternative procedures to synthesise Sn-BEA materials. Examples are the steam-assisted conversion of stannosilicate gels or the solid-/liquid-/gas-phase incorporation of Sn atoms into a dealuminated beta zeolite.[5]

The potential of another tin-containing zeolite, *i.e.* Sn-MFI, which can be crystallised in few days through an industrially-amenable hydroxide route,[6,7] has been explored only hardly so far. This is likely due to the smaller pore size in the MFI framework (5.5-6 Å) compared to the BEA (6.5-7 Å), which imposes severe diffusional constraints to pentoses and access limitations to hexoses or larger molecules.[6] Accordingly, the successful application of Sn-MFI to the conversion of bulky substrates is contingent upon the possibility to enhance its accessibility by tuning of the porous properties.

A few academic groups have investigated the production of mesoporous Sn-MFI by bottom-up approaches for application to Baeyer-Villiger oxidations. For instance, Jinka *et al.* have reported the microwave-assisted formation of hierarchical Sn-MFI from a stannosilicate gel containing carbon particles as a hard template,[8] and Luo *et al.* have produced 2 nm-thick Sn-MFI nanosheets using a non-commercial organic structure directing agent.[9] In the latter case, tin atoms were incorporated at tetrahedral framework positions and the material displayed comparable oxidation activity to Sn-MCM-41. With regards to top-down strategies to introduce mesoporosity into Sn-MFI, treatments in alkaline media have not been attempted so far. Actually, while desilication of aluminosilicates has been thoroughly explored,[10] very little is generally known about the behaviour of tetravalent metal-containing zeolites in NaOH solutions. A study on the desilication of TS-1 has been reported, which has evidenced the formation of some extraframework

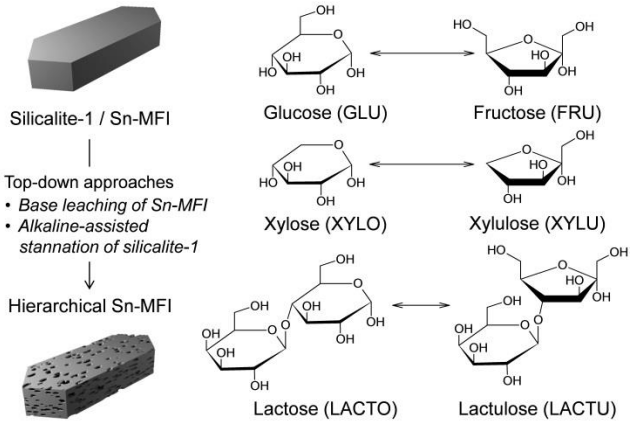

Scheme 1 Top-down strategies followed for the preparation of hierarchical Sn-containing MFI zeolites (left) and scope of application of these novel catalysts in the isomerisation of sugars (right).

titania upon the modification.[11] Owing to the simplicity and scalability of base leaching,[12] the assessment of its potential for the preparation of mesoporous Sn-MFI is appealing. An alternative top-down strategy to attain hierarchical Sn-MFI, *i.e.* alkaline-assisted stannation of silicalite-1, has been recently introduced by our group.[13] We have demonstrated that through this facile preparation, consisting in a base treatment in the presence of a soluble tin salt, tetra-coordinated Lewis-acid sites are introduced into the MFI framework which show equivalent acid strength and a striking structural resemblance to those in hydrothermally-synthesised Sn-MFI. Concomitantly, intracrystalline mesoporosity has been developed. The material has proved highly active and stable for the liquid-phase isomerisation of glyoxal to glycolic acid and alkyl glycolates in water and alcohols, respectively.[13] Still, owing to the small size of the substrate, the beneficial effect of the presence of a mesoporous network on the catalyst efficiency could not be highlighted. This should be clearly manifested when processing bulkier substrates.

In this study, we describe the preparation of mesoporous tin-containing MFI-type zeolites by (*i*) direct alkaline treatment of hydrothermally-synthesised Sn-MFI and (*ii*) alkaline-assisted stannation of silicalite-1. The latter protocol is herein optimised to minimise the content of Sn introduced in the catalysts by varying parameters such as the strength of the alkaline solution and the amount of tin precursor. The materials obtained are evaluated in the isomerisation of glucose and of other relevant sugar feedstocks such as xylose and lactose (Scheme 1). Their performance is rationalised through characterisation of their porous and structural properties.

2 Experimental

2.1 Catalyst synthesis

Parent zeolites (code P) comprised a commercial silicalite-1 (MFI, HSZ890 H0A, Tosoh) and tin-containing MFI zeolites synthesised under hydrothermal conditions following the protocols by Mal *et al*. using hydroxide or fluoride ions (denoted hereafter Sn-MFI and F-Sn-MFI, respectively) as mineralising agents.[7] In the first case, tetraethyl orthosilicate (TEOS, 93.7 g, Sigma-Aldrich, 98%) was mixed with a solution of $SnCl_4{\cdot}5H_2O$ (1.26 g, Sigma-Aldrich, 98%) in deionised H_2O (30 g) and allowed to react for 30 min under stirring. Then, tetrapropylammonium hydroxide (TPAOH, 198 g, Alfa Aesar, 20 wt.%) was added drop-wise and the mixture was stirred for 1 h. Finally, 84 g of deionised H_2O were added and the solution was stirred for 30 min. The final sol, having a molar ratio of 0.008 SnO_2: 1 SiO_2: 0.44 TPAOH: 34.3 H_2O, was transferred into a 500-cm^3 Teflon-lined autoclave and heated at 433 K for 3 days under static conditions. In the second case, a solution of $SnCl_4{\cdot}5H_2O$ (1.25 g) in deionised H_2O (50 g) was added drop-wise and under rapid stirring to a solution of NH_4F (26.75 g, Acros, 98%) in deionised H_2O (125 g). Thereafter, a solution of tetrapropylammonium bromide (TPABr, 49 g, ABCR, 98%) in deionised H_2O (280 g) was slowly added to the mixture, which was then stirred for 30 min. Finally, 43 g of fumed silica (Sigma-Aldrich) were added and the resulting sol (molar ratio: 0.005 SnO_2 : 1 SiO_2 : 0.26 TPAOH: 1 NH_4F : 35 H_2O) was stirred for 3 h. The sol was transferred into a 500-cm^3 Teflon-lined autoclave and heated at 473 K for 6 days under static conditions. The Sn-MFI crystals resulting from the two procedures were separated by filtration, washed thoroughly with deionised water, dried overnight at 338 K, and calcined in static air at 823 K (5 K min^{-1}) for 5 h to ensure the complete removal of the organic structure directing agent.

The calcined zeolites were used for post-synthetic modifications in aqueous NaOH solutions (0.02-0.2 M, 30 cm^3 per gram of dried zeolite) at 338 K for 30 min in an Easymax™ 102 reactor (Mettler Toledo). For the treatment of silicalite-1, 0.005 or 0.02 M of $SnCl_4{\cdot}5H_2O$ or $SnSO_4$ (Acros, 98%) were dissolved in the alkaline solution. After filtration, the metallosilicates were dried at 338 K overnight and calcined in static air at 823 K (5 K min^{-1}) for 5 h. These samples are denoted by the codes Sn-MFI-AT*x* and MFI-AT*x*Sn*x*C/MFI-AT*x*Sn*x*S (in which *x* corresponds to 1/10 of the molarity of the hydroxide and tin ions in the solutions and C or S indicate whether $SnCl_4{\cdot}5H_2O$ or $SnSO_4$ was used as the metal source).

Reference catalysts comprised SnO_2 (Sigma-Aldrich, 99.9%), $SnCl_4{\cdot}5H_2O$, $SnSO_4$, and a tin-containing MFI zeolite prepared by dry impregnation of a hierarchical silicalite-1 (generated with a solution of 0.2 M NaOH containing 0.005 M TPABr, according to the method described in [14]) with $SnCl_4{\cdot}5H_2O$ (0.27 wt.% Sn).

2.2 Characterisation

The content of Si and Sn in the catalysts and in selected filtrates obtained after catalyst preparation was determined by inductively coupled plasma optical emission spectroscopy (ICP-OES) using a Horiba Ultra 2 instrument equipped with a photomultiplier tube detector. Prior to the measurements, the materials were digested in an acidic mixture ($HCl/HNO_3/HF$) under heating (343 K, overnight). Nitrogen sorption at 77 K was performed using a Quantachrome Quadrasorb-SI analyser on degassed samples (10^{-1} mbar, 573 K, 3 h). Powder X-ray diffraction (XRD) was measured using a PANalytical X'Pert PRO-MPD diffractometer with Ni-filtered Cu Kα radiation ($\lambda = 0.1541$ nm). Data was recorded in the 5-70° 2θ range with an angular step size of 0.05° and a counting time of 7 s per step. Scanning electron microscopy (SEM) was carried out using a Zeiss Gemini 1530 FEG microscope operated at 2 kV on Pt-coated samples (2 nm).

Transmission electron microscopy (TEM) was undertaken using a FEI Tecnai F30 microscope operated at 300 kV (field emission gun). The samples were prepared by depositing a few droplets of zeolite suspension in methanol onto a carbon-coated copper grid, followed by evaporation at room temperature. UV-Vis spectroscopy was performed using a Varian Cary 4000 UV-Vis spectrometer in diffuse reflectance mode and barium sulphate for the background collection. Prior to the analysis, the samples were dried at 573 K for 3 h under vacuum (10^{-1} mbar). X-ray photoelectron spectroscopy (XPS) was conducted using a Physical Electronics (PHI) Quantum 2000 X-ray photoelectron spectrometer with monochromatic Al Kα radiation, generated from an electron beam operated at 15 kV and 32.3 W, and with a hemispherical capacitor electron-energy analyser equipped with a channel plate and a position-sensitive detector. The samples were firmly pressed onto indium foil patches, which were then mounted onto a sample platen and introduced into the spectrometer. The analysis was conducted at 8.10^{-9} mbar, with an electron take-off angle of 45°, and operating the analyser in the constant pass energy mode, and was repeated after sputtering the samples with 4 kV Ar^+ ions rastered over 2 × 2 mm for five minutes. As the ion etch rate was calibrated to be 20.0 nm min^{-1} for a 100-nm thick Ta_2O_5 reference film, this treatment removed *ca*. 100 nm of material from the samples. Elemental concentrations were calculated in atomic percent from the photoelectron peak areas after Shirley background subtraction and applying the built-in PHI sensitivity factors. Fourier transform infrared (FTIR) spectroscopy was performed using a Bruker Optics Vertex 70 spectrometer equipped with a high-temperature DRIFT cell (Harrick) and an MCT detector. Spectra were recorded in the range of 4000-400 cm^{-1} under N_2 flow and at 473 K by co-addition of 200 scans with a nominal resolution of 4 cm^{-1}. Prior to the measurements, the samples were dried at 673 K under N_2 flow for 4 h.

2.3 Catalytic tests

Batch catalytic tests were performed under autogenous pressure in 15-cm^3 thick-walled glass vials (Ace, pressure tubes, front seal) dipped in an oil bath heated at 353 K. The vials were loaded with 120 mg of substrate, consisting in either glucose (GLU, ABCR, 99%), xylose (XYLO, Sigma-Aldrich, 99%) or lactose (LACTO, Sigma-Aldrich, 99%), 80 mg of catalyst, and 3.88 g of water. The mixture was allowed to react under vigorous stirring for 0.25-2 h. Then, the reaction was quenched using an ice bath and the catalyst removed by means of a Chromafil Xtra 0.25 µm syringe filter. Reusability tests were performed over MFI-AT1Sn005C at 353 K and for 2 h in water, methanol (Sigma-Aldrich, 99.8%), and ethanol (Fluka, 99.8%) using glucose as the substrate. For comparative purposes, recycling tests were also conducted over the same catalyst at 363 K and for 24 h in water using glyoxal (4 wt.%, ABCR 40 wt.% aqueous solution) as the substrate. Between each run, the used catalyst was calcined under flowing air at 823 K (5 K min^{-1}) for 5 h.

Glucose, fructose (FRU, Sigma-Aldrich, 99%), mannose (MAN, Sigma-Aldrich, 99%), xylose, xylulose (XYLU), lyxose (LYXO, Sigma-Aldrich, 99%), lactose, and lactulose (LACTU, Sigma-Aldrich, 95%) were isolated by high-performance liquid chromatography (HPLC) in a Merck LaChrom system equipped with a Biorad Aminex HPX-87C column heated at 353 K and a refractive index detector (Hitachi Chromaster model 5450) set at 303 K, using water (0.5 mL min^{-1}) as the eluent. Quantification was obtained by integration of their respective peaks using butan-2-one (Merck, 99.5%) as an internal standard. The conversion of the substrate was calculated as the mole of substrate reacted divided by the mole of substrate fed, whereas the product yield as the mole of product formed divided by the initial moles of substrate. In the case of xylulose, the yield was calculated using the response factor of xylose.

3 Results and discussion

3.1 Hierarchical Sn-MFI zeolites

The generation of mesoporous Sn-MFI was firstly approached *via* the direct alkaline treatment of hydrothermally-synthesised materials. Parent zeolites were prepared both through the hydroxide route (Sn-MFI-P) and in the presence of fluoride ions (F-Sn-MFI-P). As visualised by SEM (Fig. 1), Sn-MFI-P consisted of agglomerated spherical crystals with a diameter of *ca*. 200 nm. Differently, F-Sn-MFI-P featured large and uniform coffin-like crystals of 15-20 µm length and 4 µm width, sometimes exhibiting intergrowth. For both zeolites, FTIR spectroscopy of the OH stretching region (Fig. 2) revealed absorption bands associated with terminal (3722 and 3693 cm^{-1}) and hydrogen-bonded internal (3500 cm^{-1}) silanols.[5] The substantially lower intensity of all of the bands for F-Sn-MFI-P supports the more regular surface termination of the crystals of this sample compared to Sn-MFI-P. These results are in line with previous evidence that the use of hydroxide ions leads to small and highly defective crystals, while that of fluoride ions to large and defect-free crystals, similarly to the case of Sn-BEA.[7,15,16] The composition and textural properties of the two zeolites are reported in Table 1 (entries 1,3). Both samples possessed an external surface area (S_{meso}) of 20-50 m^2g^{-1} and a micropore volume (V_{micro}) of 0.14-0.16 cm^3 g^{-1}, as typically observed for ZSM-5 zeolites. These parent materials were modified by treatments with aqueous NaOH solutions. In the case of F-Sn-MFI, no development of mesoporosity was observed upon base leaching in 0.2 M NaOH (Table 1, entry 2). This result is not surprising, as the absence of surface defects and/or grain boundaries has been shown to be detrimental in order to initiate the dissolution process of high-silica zeolites.[17] Contrarily, the S_{meso} of Sn-MFI-AT*x* samples progressively increased with the strength of the NaOH solution applied, reaching a maximum (133 m^2g^{-1}) with Sn-MFI-AT1 (Table 1, entries 4-6, and Fig. 3a).

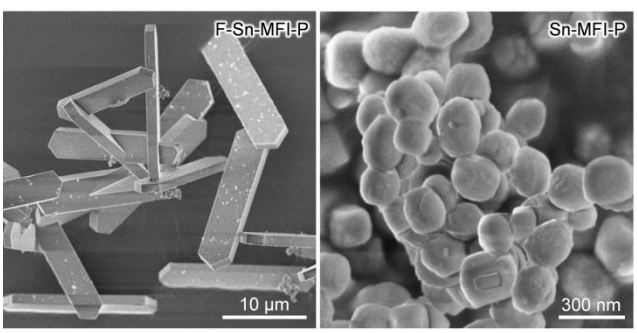

Fig. 1 SEM micrographs of Sn-MFI synthesised in fluoride (left) and hydroxide media (right).

Table 1 Composition and textural properties of the Sn-containing catalysts studied in this work.

Entry	Catalyst[a]	Yield[b] (%)	Crystallinity[c] (%)	Si/Sn[d] (mol mol^{-1})	Sn content[d] (wt.%)	V_{micro}[e] (cm^3 g^{-1})	S_{meso}[e] (m^2 g^{-1})	V_{pore}[f] (cm^3 g^{-1})
1	F-Sn-MFI-P	100	100	114	1.83	0.16	20	0.19
2	F-Sn-MFI-AT2	86	99	116	1.82	0.16	15	0.18
3	Sn-MFI-P	100	100	156	1.26	0.14	49	0.27
4	Sn-MFI-AT02	97	98	167	1.20	0.13	72	0.30
5	Sn-MFI-AT05	93	80	158	1.28	0.13	90	0.25
6	Sn-MFI-AT1	81	64	139	1.37	0.12	133	0.35
7	Sn-MFI-AT2	48	65	120	1.64	0.12	108	0.36
8	MFI-P	100	100	–	–	0.14	54	0.22
9	MFI-AT1Sn005C	90	84	760	0.26	0.14	75	0.23
10	MFI-AT2Sn02C	87	75	141	1.35	0.11	98	0.24
11	MFI-AT1Sn005S	82	84	497	0.41	0.12	76	0.22
12	MFI-AT2Sn02S	70	55	101	2.04	0.09	131	0.30
13	MFI-AT2TPA-DI	85	58	716	0.27	0.07	141	0.37

[a] P = parent, AT*x* = alkaline-treated in the presence of 0.*x* M of NaOH, Sn*x*C / Sn*x*S = alkaline-treated in NaOH in the presence of 0.*x* M of $SnCl_4 \cdot 5H_2O$ / $SnSO_4$ respectively. [b] Based on the amount of solid recovered after alkaline treatment, ion-exchange, and calcination. [c] Derived from XRD. [d] Determined by ICP-OES analysis. [e] Determined by the *t*-plot method. [f] Volume adsorbed at $p/p_0 = 0.99$.

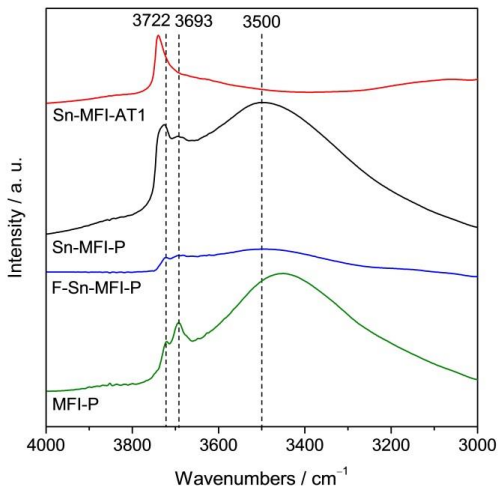

Fig. 2 FTIR spectra of the OH stretching region of MFI-P, F-Sn-MFI-P, Sn-MFI-P, and Sn-MFI-AT1.

Pore size distribution analysis indicated the formation of mesopores in the 5-20 nm range (Fig. 3a), which were visualised by TEM (Fig. 3b). Noteworthily, a higher NaOH concentration (0.2 M, Sn-MFI-AT2) led to a lower S_{meso} (108 m^{2}g^{-1}, Table 1, entry 7). The crystallinity of the zeolitic structure was substantially retained even upon application of the more concentrated solutions (Fig. 3c). In addition, the alkaline treatment appeared to reduce the defectivity of the zeolite surface. In fact, the broad OH stretching band associated with hydrogen-bonded internal silanols visible in the FTIR spectrum of Sn-MFI-P vanished upon base leaching (Fig. 2). Such a behaviour is characteristic of vacancy healing processes and has already been reported in relation to the post-synthetic modification of dealuminated zeolite beta.[5] Interestingly, no major alteration was detected in the Si/Sn ratio, which only slightly decreased from 156 (P) to 139 (AT1). In contrast to alkaline treatment of aluminium-containing ZSM-5 zeolites, in which silicon is preferentially removed,[10] this result implies that Si and Sn are similarly prone to leaching in the presence of a base. Indeed, comparable Si/Sn ratios were determined for the filtrates obtained after the treatment (*e.g.*, 140 and 159 for Sn-MFI-AT0.5 and Sn-MFI-AT1, respectively). The latter observation points to a clear intrinsic drawback of base leaching as a route to hierarchical Sn-MFI, as a substantial amount of potential active sites is lost upon the modification.

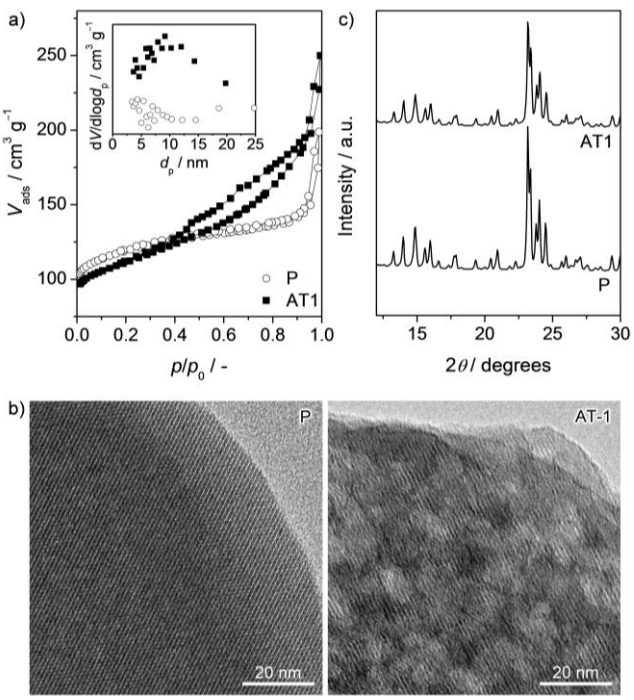

Fig. 3 (a) N_2 sorption isotherms, (b) transmission electron micrographs and (c) X-ray diffraction patterns of Sn-MFI in parent form (P) and after alkaline treatment in the presence of 0.1 M NaOH (AT1). The inset in (a) depicts the BJH mesopore size distributions.

A protocol recently described by our group,[13] *i.e.* alkaline-assisted stannation, was applied as an alternative route to superior mesoporous Sn-MFI zeolites. In fact, several advantages seemed to be related to this approach. Firstly, it already generated mesoporous catalysts exhibiting outstanding activity, selectivity, and stability. Secondly, the utilisation of Sn in the catalyst is

Table 2 Catalytic data for the isomerisation of glucose over Sn-containing catalysts after 15 min or 2 h (in brackets) of reaction.

Entry	Catalyst[a]	Glucose conversion (%)	Fructose yield (%)	Mannose yield (%)	Fructose selectivity (%)	Total saccharides[b] (%)
1	Sn-MFI-P	0(0)	0(0)	0(0)	n.a.	100(100)
2	Sn-MFI-AT1	13(35)	9(24)	0(2)	65(66)	96(91)
3	MFI-P	0(0)	0(0)	0(0)	n.a.	100(100)
4	MFI-AT1Sn005C	16(35)	13(25)	1(3)	84(72)	98(93)
5	MFI-AT2Sn02C	20(37)	18(27)	1(3)	91(73)	99(93)
6	MFI-AT1Sn005S	13(41)	10(26)	1(3)	80(63)	98(88)
7	MFI-AT2Sn02S	21(38)	17(24)	0(3)	80(65)	96(89)
8	MFI-AT2TPA-DI	13(38)	10(24)	0(3)	75(64)	97(89)

[a] P = parent, AT*x* = alkaline-treated in the presence of 0.*x* M of NaOH, Sn*x*C/Sn*x*S = alkaline-treated in NaOH in the presence of 0.*x* M of $SnCl_4 \cdot 5H_2O$/$SnSO_4$. [b] Calculated as the sum of glucose, fructose, and mannose after reaction.

expected to be highly enhanced, since zeolite metallation in alkaline media has shown to lead to the preferential incorporation of the metal at the external surface of the material, which is the only accessible area in the application under study. Thirdly, as the metal is introduced post synthesis, the flexibility of this protocol is higher compared to the alkaline treatment, enabling to tune the porous properties as well as the metal content in the material. The original recipe comprised the treatment of silicalite-1 in a 0.3 M NaOH solution saturated with tin sulphate. As the deriving material contained a rather high amount of tin (*ca.* 2.55 wt.%) and a filtration step prior to the alkaline-assisted stannation was required to remove the undissolved $SnSO_4$,[13] the alkaline strength and the nature and concentration of the salt used as the tin precursor were herein varied upon application of this method. Experimentally, two different sets of conditions were employed: (*i*) a 0.1 M NaOH solution containing 0.005M of $SnCl_4$ or $SnSO_4$ and (*ii*) a 0.2M NaOH solution containing 0.02M of $SnCl_4$ or $SnSO_4$. The composition and textural properties of the samples obtained are reported in Table 1 (entries 9-12). According to the elemental analysis, MFI-AT1Sn005S and MFI-AT2Sn02S contained 1.5 times more metal than MFI-AT1Sn005C and MFI-AT2Sn02C, respectively, indicating that the use of tin sulphate results in a higher tin incorporation efficiency compared to that of tin chloride. Furthermore, a lower solid yield and a more pronounced development of mesoporosity were associated with the application of the former salt, as exemplified by the cases of MFI-AT2Sn02S and MFI-AT2Sn02C (Table 1, entries 10,12). Although no in-depth investigation has been performed on the influence of the type of counter-ion on the desilication and alkaline-assisted metallation processes so far, these findings are in line with our previous evidence regarding the effect of the presence of a salt during base leaching.[18] Considering the greater solubility of tin chloride and the lower basicity of the alkaline solution containing it compared to the case of tin sulphate (pH = 12.67 *versus* 12.95), the differences described above might originate from the distinct alkalinity and/or ionic strength of the solutions. The exact determination of the impact of these parameters on the catalyst properties is not trivial and lies beyond the scope of this study.

3.2 Sugar isomerisation

Firstly, the access- and equilibrium-limited isomerisation of glucose to fructose was investigated. A relatively low reaction temperature (353 K) was selected in order to minimise the unavoidable thermal degradation of both the substrate and the product. Over Sn-MFI-P, no conversion was observed at early stages or even after 2 h of reaction of a 3 wt.% solution of glucose, as shown in Fig. 4a and Table 2 (entry 1). A similar result was observed for F-Sn-MFI-P. This evidence is in line with previous reports and relates to the insufficient amount of tin sites located at the external surface of the zeolite.[6] Over alkaline-treated samples (Sn-MFI-AT*x*), fructose was already produced after 15 min of reaction. Its yield gradually augmented (to 8%) with the increase of S_{meso} until the latter reached a value of 90 m^2g^{-1}, remaining at a similar level for larger mesoporous surface areas (Fig. 5). Accordingly, a moderate increase in S_{meso} seemed sufficient to boost the amount of accessible active tin centres. Unfortunately, a direct correlation between performance and number of actual catalytic sites is difficult to establish. The total amount of tin atoms at the external surface could be estimated by employing a probe molecule, such as lutidine, which cannot access the micropores of the MFI zeolite. Nevertheless,

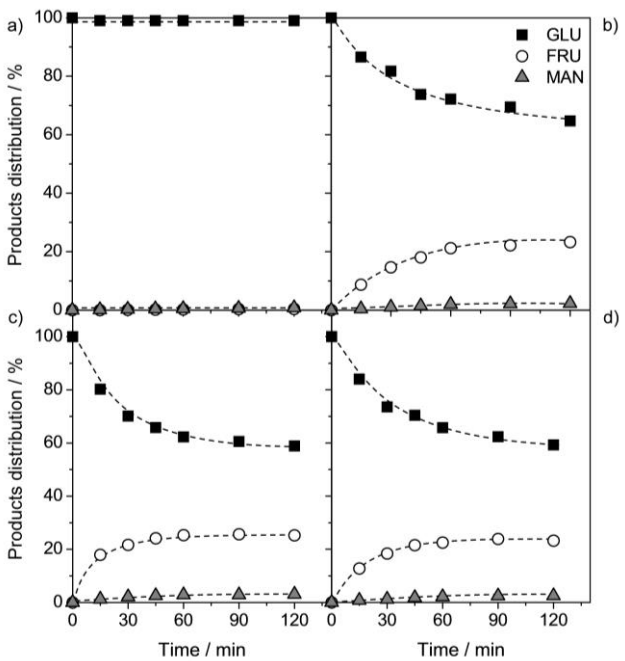

Fig. 4 Temporal evolution of the glucose conversion and the fructose and mannose yields over (a) Sn-MFI-P, (b) Sn-MFI-AT1, (c) MFI-AT2Sn02C, and (d) MFI-AT1Sn005C.

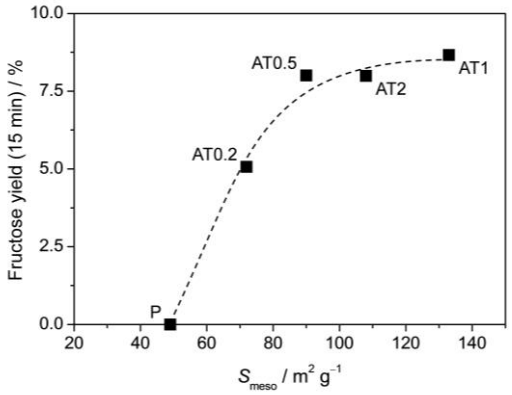

Fig. 5 Yield of fructose after 15 min of reaction versus the mesoporous surface area of the samples generated upon alkaline treatment of Sn-MFI-P.

this value might not coincide with the number of sites effectively relevant for the catalytic process, as the alkaline treatment might have generated Sn species with non-equivalent properties (*vide infra*). The modified catalyst featuring the highest mesoporosity, Sn-MFI-AT1, was evaluated in glucose isomerisation during a longer reaction time. The fructose yield progressively increased, attaining a plateau value of *ca*. 24% after 1 h (Fig. 4b). Only a minor amount of mannose concomitantly formed, highlighting the high catalyst selectivity in this reaction. Glucose degradation was responsible for the further slight enhancement of the conversion after this time.

With regards to the zeolites prepared by alkaline-assisted stannation, a kinetic profile was initially collected for MFI-AT2Sn02C, as this catalyst contains a similar tin content to Sn-MFI-AT1 (Fig. 4c). The yield of fructose was 18% after 15 min and reached a plateau value of 27% after 2 h, corresponding to a fructose selectivity of 72% (Fig. 4c, Table 2, entry 5). These values are clearly higher than for the alkaline-treated sample. Interestingly, the Sn-richer MFI-AT2Sn02S zeolite displayed only comparable fructose yields and a moderately lower selectivity with respect to MFI-AT2Sn02C (Table 2, entry 7). A remarkable performance was also observed for the stannated catalysts containing a reduced amount of tin. The increase in fructose yield with reaction time was only slightly slower for MFI-AT1Sn005C (0.26 wt.% Sn) and almost the same value (25%) was reached after 2 h (Table 2, entry 4, Fig. 4d). As for the catalysts richer in Sn, the material prepared with tin sulphate was somewhat inferior to that obtained using tin chloride (Table 2, entry 6). The substantial retention of the activity upon reducing the tin content goes along with a recent study by Dijkmans *et al.* reporting that Sn-beta prepared by dealumination and ion exchange gives rise to an equal or higher turn-over-frequency compared to hydrothermally-prepared Sn-beta despite the twice lower tin content.[5d] The origin of the different performance of the catalysts prepared by alkaline treatment and by alkaline-assisted metallation will be tackled in the following through characterisation studies.

In view of supporting the superiority of alkaline-assisted stannation in generating highly performing Lewis-acid centres, a catalyst prepared by simple dry impregnation with tin chloride (0.27 wt.% of Sn, Table 1, entry 13) of a hierarchical silicalite-1, synthesised according to a well-established method,[14] was assessed. This zeolite displayed fructose yields at 15 min and 2 h (Table 2, entry 8) which were slightly lower compared to those of the sample stannated with tin chloride and having a similar metal loading and its selectivity was clearly inferior. While this outcome confirms the higher suitability of the base-aided post-synthetic treatment, the activity of the impregnated catalyst was surprising due to the known [2a] and experimentally confirmed inability of bulk SnO_2 to isomerise glucose. In this respect, it is suggested that, upon impregnation and calcination, at least part of the tin deposited was activated upon migration into the vacancies present in the hierarchical silicalite-1, which is highly defective due to the base treatment to introduce mesoporosity. Dijkmans *et al* actually used vacancy creation and healing as an alternative method to synthesise Sn-beta,[5d] and an analogous situation was evidenced in the case of Ga-containing USY zeolites developed for the isomerisation-esterification of dihydroxyacetone to alkyl lactates.[19] Additionally, the intrinsic activity of a well-dispersed and, thus, highly defective SnO_2 phase cannot be excluded.

Other bulky sugars including xylose (*i.e.* pentose) and lactose (*i.e.* disaccharide) were evaluated as substrates for isomerisation. [2b,3b] The reactions were conducted under the same conditions as described above and initially over Sn-MFI and the hierarchical MFI-AT1Sn005C catalyst. When studying xylose conversion, the yield of xylulose was found to progressively increase throughout the 2 h of reaction up to 8% (Fig. 6a) for the hydrothermally-prepared zeolite. The fact that no steady state was reached highlights the diffusion-limited nature of this transformation. The competitive epimerisation of xylose to lyxose was also favoured over Sn-MFI, as the yield of this by-product reached 4% during the test. A much faster conversion was observed over MFI-AT1Sn005C (Fig. 6b) and a maximum xylulose yield was already attained after 30 min of reaction. Interestingly, lower lyxose yields were observed over this sample. The use of a hierarchical Sn-MFI clearly alleviated the diffusion constraints and unexpectedly also increased the selectivity of the process. The latter might be the consequence of the partly different nature of the Sn sites in the stannated zeolite (*vide infra*). Chemical approaches, *i.e.* modification of the active sites by changing the type of solvent or by adding inorganic salts, have already been demonstrated successful to steer the epimerisation/isomerisation selectivity in zeolites.[20,21]

With respect to lactose isomerisation, no conversion was observed over Sn-MFI-P, as anticipated from the greater

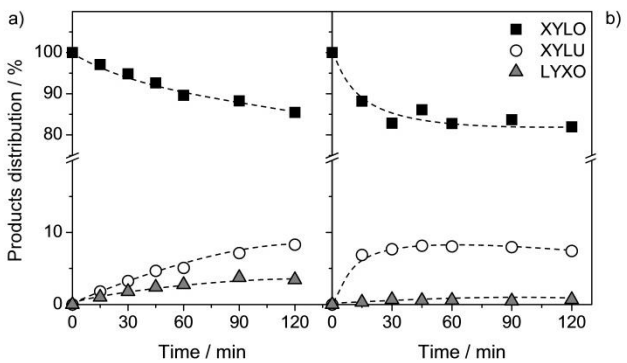

Fig. 6 Temporal evolution of the xylose conversion and the xylulose and lyxose yields over (a) Sn-MFI-P and (b) MFI-AT1Sn005C.

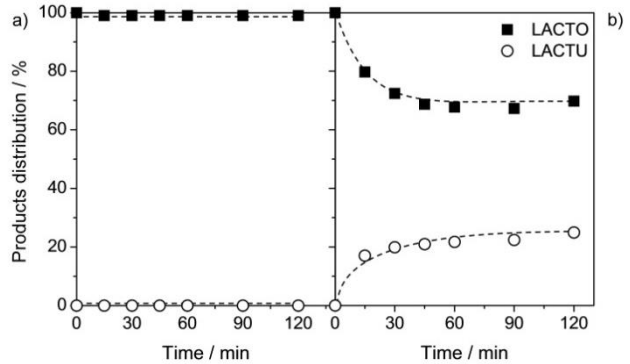

Fig. 7 Temporal evolution of the lactose conversion and the lactulose yield over (a) Sn-MFI-P and (b) MFI-AT1Sn005C.

bulkiness of this substrate (Fig. 7a), while the utilisation of MFI-AT1Sn005C proved to succeed in circumventing the access limitation also for a disaccharide. In fact, yields of lactulose of 17% and 24% were observed after 15 min and 2 h of reaction (Fig. 7b). As these values match those of the fructose yield from glucose, it is deduced that this sugar has the same reactivity regardless of the fact that it constitutes an independent unit or is linked to another sugar.

Catalytic data for the isomerisation of these additional substrates were also collected over Sn-MFI-AT1 to obtain an overview of the behaviour of the two types of hierarchical zeolites in the transformation of diffusion- and access-limited sugars (Table SI1). The results were analysed to derive a descriptor for the enhancement of the conversion upon use of either of the mesoporous materials compared to the purely microporous Sn-MFI. Firstly, the parameter α was calculated by relating the product yield over each modified catalyst after 15 min and 2 h with respect to that over Sn-MFI after the same reaction times (Fig. SI1). Then, the values obtained for the alkaline-treated material were subtracted from those determined for the stannated catalyst, *i.e.* $\beta = \alpha$(MFI-AT1Sn005C) – α(Sn-MFI-AT1). The figures obtained are plotted against the Stokes diameter of each substrate in Fig. 8. The increasing value of β from xylose to glucose and lactose indicates that alkaline-assisted stannation is a more advantageous method than alkaline-treatment for the preparation of Sn-containing mesoporous catalysts for sugar isomerisation and especially in view of the conversion of access-limited substrates.

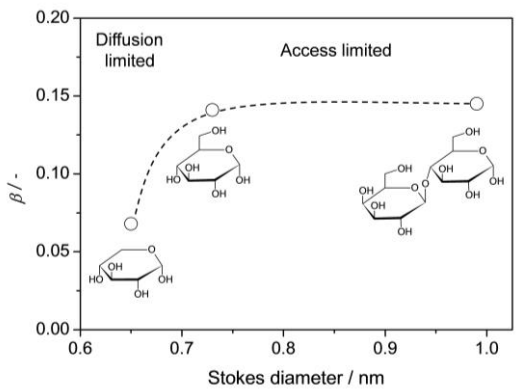

Fig. 8 Difference in isomerisation efficiency (β) between Sn-MFI-AT1 and MFI-AT1Sn005C *versus* the Stokes diameter of the substrates.

3.3 Characterisation of tin species

In order to understand the difference in performance among the hierarchical tin-containing MFI catalysts prepared by top-down approaches as well as the influence of the nature of the tin precursor used during alkaline-assisted stannation, the structure of the tin sites was investigated by diffuse reflectance UV-Vis spectroscopy. Sn-MFI-P and Sn-MFI-AT1 produced similar spectra, displaying a sharp band centred at 208 nm, typically associated with the band-gap energy of tin tetra-coordinated to four oxygen atoms and usually related to tin embedded into the zeolite framework (Fig. 9a).[20] This evidence indicates that the original structure of the Sn sites was mainly retained upon alkaline treatment, although the presence of a minority of centres featuring a different nature cannot be excluded. In the case of the samples prepared by alkaline-assisted stannation (Fig. 9b), the band at 208 nm still dominates the spectrum but an additional feature at 234 nm is visible, which is usually attributed to small SnO_2 domains.[20] In line with our previous study on stannated MFI catalysts,[13] this suggests that part of the tin is fully integrated into the framework and part has a different chemical structure, which seems to be catalytically less relevant. Considering the distinct relative intensity of the two features, a lower fraction of framework tin is present in the zeolite prepared with tin sulphate. The spectrum of the sample prepared by dry-impregnation of tin chloride on the hierarchical silicalite-1 is comparable to that of MFI-AT1Sn005S with respect to the bands present and their relative intensity. This evidence supports our previous speculation about the origin of the activity of this catalyst.

As the greatly higher proportion of Sn-MFI-like sites in the alkaline-treated material compared to the stannated and impregnated catalysts did not reflect into a superior performance, the surface tin concentration seemed to play a critical role. Aiming at unravelling its effect, Sn-MFI-P, Sn-MFI-AT1, MFI-AT2Sn02C were analysed by XPS (Table 3). The latter catalyst was selected instead of MFI-AT1Sn005C owing to its comparable bulk Sn content with respect to the other two samples. A *ca.* 7 times higher value (Table 3) was obtained for this zeolite, confirming that alkaline assisted-metallation led to an enrichment of the active metal at the surface, which positively influenced the catalyst activity. This was further confirmed by repeating the analysis after removal of a *ca.* 100 nm-thick layer

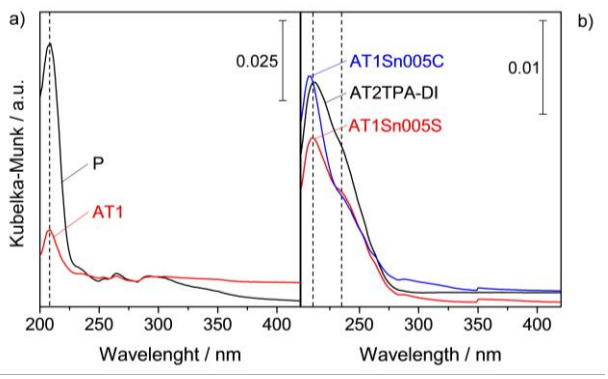

Fig. 9 DR-UV-Vis spectra of (a) Sn-MFI in parent form and after alkaline treatment and (b) hierarchical Sn-containing zeolites prepared by post-synthetic treatment of silicalite-1.

Table 3 Atomic concentration of O, Si, and Sn in the samples as determined by XPS analysis

Catalyst	Atomic concentration (%)		
	O 1s	Si 2p	Sn 3d
Sn-MFI-P	65.80	29.01	0.40 (0.18)[a]
Sn-MFI-AT1	66.36	29.21	0.55 (0.22)
MFI-AT2Sn02C	65.75	25.92	3.18 (0.31)

[a] Values obtained after removing a *ca.* 100 nm-thick layer of the sample by sputtering with 4kV Ar^+ ions at a rate of 20 nm min^{-1}.

from the materials by sputtering with Ar^+ ions. A dramatic drop in Sn content was in fact observed for the stannated catalyst, while the change was moderate for the other systems. It is reasonable to assume that metallation with $SnSO_4$ and $SnCl_4{\cdot}5H_2O$ determined a similar tin distribution and that the difference in activity between the two catalysts mainly depends on the distinct ratio of tin sites highlighted by UV-Vis spectroscopy. The comparably high activity of MFI-AT2TPA-DI indicates that deposition of Sn at the external surface of the zeolite was also favoured upon dry impregnation.

The two strategies herein developed to prepare hierarchical tin-containing materials are graphically summarised in Scheme 2 in relation to the access-limited glucose isomerisation. While the introduction of intracrystalline mesoporosity into Sn-MFI increases the fraction of tin sites accessible to the reactant, most of the metal remains located in the micropores of the zeolite and, thus, is unexploited. In contrast, stannation of silicalite-1 solely occurs at the external surface, which is similarly enhanced in the treatment, and, therefore, the amount of accessible tin atoms is maximal. Based on the structure-performance relationships derived above, we can conclude that the benefit of an exclusive site location at the mesopores, *i.e.* egg-shell-like distribution of the active species, greatly surpasses the drawback of site heterogeneity. Furthermore, in view of the analogous mesoporous surface, the distribution of tin appears as the critical contributor in the rationalisation of the efficiency of the two hierarchical catalysts in terms of β. Indeed, the advantage of using a stannated catalyst is greater for an access-limited reaction and slightly

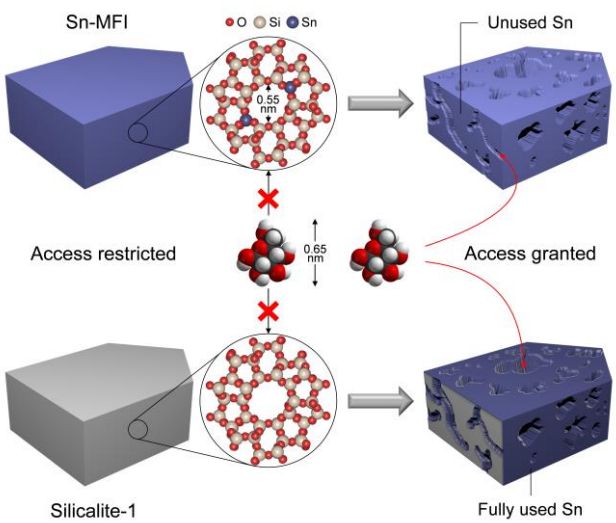

Scheme 2 Illustration of the porous features and of the distribution of the Lewis-acid tin centres in the parent and the hierarchical zeolites obtained *via* alkaline treatment and alkaline-assisted stannation.

inferior for a diffusion-limited reaction, in which the sites in the micropores are utilised to a minor extent.

3.4 Reusability study

Reusability tests were conducted over our best catalyst (*i.e.* MFI-AT1Sn005C) under the same experimental conditions as reported above. In order to eliminate the adsorbed sugar degradation products, the zeolite was regenerated by calcination in flowing air (823 K, 5 K min^{-1}, 5 h) between each run. As evidenced in Fig. 10, the FRU yield dropped from 26% to 9% in the second test. Noteworthy, the FRU selectivity increased (from 72 to 95%), as generally observed at low GLU conversion. The significant loss in activity of the catalyst was surprising considering the high stability of silicalite-1 metallated with tin sulphate in the aqueous-phase isomerisation of glyoxal.[13] In order to exclude a possible role of the nature of the tin precursor on the stability, recyclability tests for glyoxal isomerisation were repeated with MFI-AT1Sn005C. The catalyst performance was maintained in the second run (Fig. SI2).

Aiming at unravelling the deactivation mechanism upon glucose isomerisation, the spent catalyst was analysed by XRD, N_2 sorption, and ICP-OES. While the porous and structural properties of the metallosilicate were preserved (Fig. SI3), the tin content was substantially depleted (*ca.* 67%). A contribution from homogeneous catalysis to the reaction was excluded based on the observed inactivity of the tin salts used as precursors. Based on the stability of the catalyst in the glyoxal conversion, the nature of the molecules involved in the conversions rather than the aqueous medium seemed to be at the origin of the metal leaching. Both glucose and fructose indeed contain chelating groups which may aid metal extraction. Recyclability tests in methanol and ethanol evidenced a lower but still significant tin loss (40% and 36%, respectively), further supporting the substrate-dependent deactivation. The distinct extents of metal leaching might be due to the modulation of the chelating properties of the sugars through variation of the polarity of the liquid environment, *i.e.* different solvation effects.

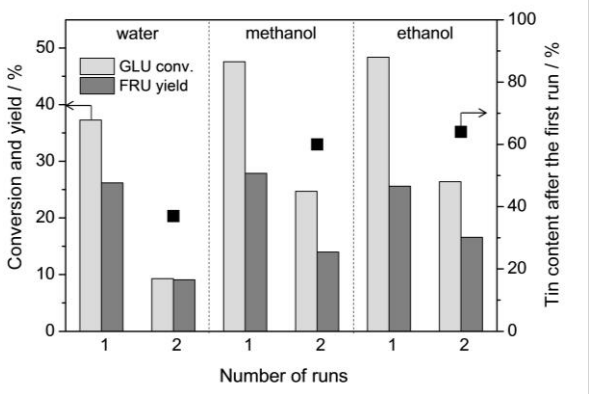

Fig. 10 GLU conversion and FRU yield obtained at 353 K and 2 h after consecutive catalytic runs in water, methanol, and ethanol and percentage of tin remaining in the catalyst after the first run.

4 Conclusions

Alkaline treatment of hydrothermally-synthesised Sn-MFI and alkaline-assisted stannation of silicalite-1 were successfully

applied as simple and scalable post-synthetic strategies to produce hierarchical Sn-containing MFI-type zeolites. These catalysts demonstrated able to isomerise a bulky sugar, such as glucose, which cannot be converted by microporous Sn-MFI because of access limitation. In spite of the heterogeneity of the tin sites introduced, the stannated catalysts proved superior compared to those produced from Sn-MFI due to the exclusive placement of the tin centres at the external surface of the zeolite, which enabled a very high metal utilisation. Thus, the amount of metal incorporated could be greatly lowered without significantly compromising the performance. The low-loaded tin-containing zeolite was shown to efficiently isomerise also the diffusion-limited xylose as well as the bulkier access-limited disaccharide lactose. The reusability of the tin-based catalysts was explored and the materials' sensitivity towards the nature of the substrate was highlighted. Such industrially-relevant aspects of catalytic conversions should be tackled in greater detail in emerging applications. Possibly, Lewis-acid metals sites less reactive than tin could have brighter perspectives to fulfil the lifetime requirements for large-scale processes.

Acknowledgments

This work was supported by the Swiss National Science Foundation (Project Number 200021-140496). The Electron Microscopy Centre of the ETH Zurich is acknowledged for the use of their facility. The authors thank T. C. Keller for the 3-D illustrations, Dr. S. J. Mitchell and N. -L. Michels for the TEM and SEM analyses, and Dr. Davide Ferri for the UV-Vis spectroscopic analysis.

Notes and references

[a] *Institute for Chemical and Bioengineering, Department of Chemistry and Applied Biosciences, ETH Zurich, Vladimir-Prelog-Weg 1, CH-8093 Zurich, Switzerland.*
[b] *Empa, Swiss Federal Laboratories for Materials Science and Technology, Überlandstrasse 129, CH-8600 Dübendorf,Switzerland.*
E-mails:cecilia.mondelli@chem.ethz.ch; jpr@chem.ethz.ch
Fax: +41 44 6331405; Tel: +41 44 6337120.

† Electronic Supplementary Information (ESI) available: calculation of the parameter α for Sn-MFI-AT1 and MFI-AT1Sn005C for xylose, glucose and lactose isomerisation; XRD and N_2 sorption data of MFI-AT1Sn005C in fresh form and after regeneration upon calcination; and catalytic data for the isomerization of xylose, glucose, and lactose over Sn-MFI-AT1 and MFI-AT1Sn005C and glyoxal isomerisation over MFI-AT1Sn005C. DOI: 10.1039/b000000x/

1 (a) E. Taarning, C. M. Osmundsen, X. Yang, B. Voss, S. I. Andersen, C. H. Christensen, *Energy Environ. Sci.*, 2011, **4**, 793; (b) M. Moliner, *Dalton Trans.*, 2014, **43**, 4197.
2 (a) M. Moliner, Y. Román-Leshkov, M. E. Davis, *Proc. Natl. Acad. Sci. U. S. A.*, 2010, **107**, 6164; (b) V. Choudhary, A. B. Pinar, S. I. Sandler, D. G. Vlachos, R. F. Lobo, *ACS Catal.*, 2011, **1**, 1724; (c) M. S. Holm, Y. Pagán-Torres, S. Saravanamurugan, A. Riisager, J. A. Dumesic, E. Taarning, *Green Chem.*, 2012, **14**, 702; (d) A. Corma, L. T. Nemeth, M. Renz, S. Valencia, *Nature*, 2001, **412**, 423; (e) Y. Román-Leshkov, M. Moliner, J. A. Labinger, M. E. Davis, *Angew. Chem., Int. Ed.*, 2010, **49**, 8954.
3 (a) T. Blasco, M. A. Camblor, A. Corma, P. Esteve, A. Martínez, C. Prieto, S. Valencia, *Chem. Commun.*, 1996, 2367; (b) R. Gounder, M. E. Davis, *J. Catal.*, 2013, **308**, 176; (c) M. Trzpit, M. Soulard, J. Patarin, N. Desbiens, F.Cailliez, A. Boutin, I. Demachy, A. H. Fuchs, *Stud. Surf. Sci. Catal.*, 2008, **174**, 561.
4 S. Valencia, A. Corma, *US Patent US5968473A*, 1999.
5 (a) P. Li, G. Liu, H. Wu, Y. Liu, J. -G. Jiang, P. Wu, *J. Phys. Chem. C*, 2011, **115**, 3663; (b) C. Hammond, S. Conrad, I. Hermans, *Angew. Chem., Int. Ed.*, 2012, **51**, 11736; (c) Z. Kang, X. Zhang, H. Liu, J. Qiu, K. L. Yeung, *Chem. Eng. J.*, 2013, **218**, 425; (d) J. Dijkmans, D. Gabriëls, M. Dusselier, F. de Clippel, P. Vanelderen, K. Houthoofd, A. Malfliet, Y. Pontikes, B. F. Sels, *Green Chem.*, 2013, **15**, 2777.
6 (a) C. M. Osmundsen, M. S. Holm, S. Dahl, E. Taarning, *Proc. R. Soc. A*, 2012, **468**, 2000; (b) C. M. Lew, N. Rajabbeigi, M. Tsapatsis, *Microporous Mesoporous Mater.*, 2012, **153**, 55.
7 N. K. Mal, V. Ramaswamy, P. R. Rajamohanan, A.V. Ramaswamy, *Microporous Mater.*, 1997, **12**, 331.
8 K. M. Jinka, S. -C. Lee, S. -E. Park, R. V. Jasra, *Stud. Surf. Sci. Catal.*, 2008, **174**, 1187.
9 H. Y. Luo, L. Bui, W. R. Gunther, E. Min, Y. Román-Leshkov, *ACS Catal.*, 2012, **2**, 2695.
10 D. Verboekend, J. Pérez-Ramírez, *Catal. Sci. Technol.*, 2011, **1**, 879.
11 A. Silvestre-Albero, A. Grau-Atienza, E. Serrano, J. García-Martínez, J. Silvestre-Albero, *Catal. Commun.*, 2014, **44**, 35.
12 R. Chal, C. Gerardin, M. Bulut, S. van Donk, *ChemCatChem*, **2011**, 3, 67.
13 P. Y. Dapsens, C. Mondelli, B. T. Kusema, R. Verel, J. Pérez-Ramírez, *Green Chem.*, 2014, **16**, 1176.
14 D. Verboekend, J. Pérez-Ramírez, *Chem. Eur. J.*, 2011, **17**, 1137.
15 C. E. A. Kirschhock, E. J. P. Feijen, P. A. Jacobs, J. A. Martens, Hydrothermal Zeolite Synthesis. Handbook of Heterogeneous Catalysis. Wiley-VCH Verlag: Weinheim, Germany, 2008, p. 164.
16 Y. Kalvachev, M. Jaber, V. Mavrodinova, L. Dimitrov, D. Nihtianova, V. Valtchev, *Microporous Mesoporous Mater.*, 2013, **177**, 127.
17 L. Sommer, D. Mores, S. Svelle, M. Stöcker, B. M. Weckhuysen, U. Olsbye, *Microporous Mesoporous Mater.*, 2010, **132**, 384.
18 D. Verboekend, J. Pérez-Ramírez, *ChemSusChem*, 2014, **7**, 753.
19 (a) P. Y. Dapsens, C. Mondelli, J. Pérez-Ramírez, *ChemSusChem*, 2013, **6**, 831; (b) P. Y. Dapsens, M. J. Menart, C. Mondelli, J. Pérez-Ramírez, *Green Chem.*, 2014, **16**, 589.
20 R. Bermejo-Deval, R. Gounder, M. E. Davis, *ACS Catal.*, 2012, **2**, 2705.
21 (a) W. R. Gunther, Y. Wang, Y. Ji, V. K. Michaelis, S. T. Hunt, R. G. Griffin, Y. Román-Leshkov, *Nat. Commun.*, 2012, **3**, 1109; (b) R. Gounder, M. E. Davis, *ACS Catal.*, 2013, **3**, 1469.

Electronic Supplementary Information

Hierarchical Sn-MFI zeolites prepared by facile top-down methods for sugar isomerisation

Pierre Y. Dapsens,[a] Cecilia Mondelli,[a]* Jakub Jagielski,[a] R. Hauert[b] and Javier Pérez-Ramírez [a]*

[a]*Institute for Chemical and Bioengineering, Department of Chemistry and Applied Biosciences, ETH Zurich, Vladimir-Prelog-Weg 1, CH-8093 Zurich, Switzerland. Fax: +41 44 6331405 Tel: +41 44 6337120; E−mails: cecilia.mondelli@chem.ethz.ch; jpr@chem.ethz.ch.*

[b]*Empa, Swiss Federal Laboratories for Materials Science and Technology, Überlandstrasse 129, CH-8600 Dübendorf, Switzerland.*

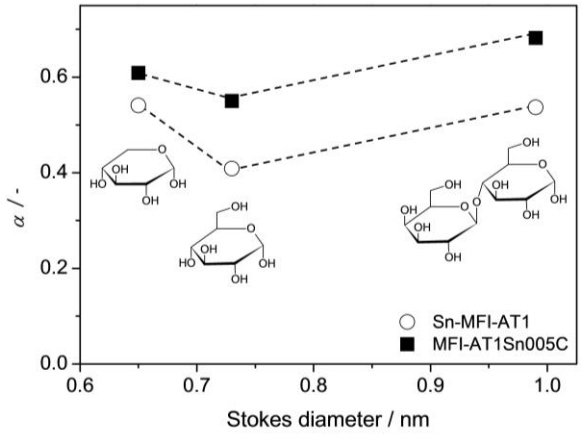

Fig. SI1 α (defined below) *versus* the Stokes diameter of the substrates for catalysts prepared *via* alkaline-treatment (Sn-MFI-AT1) and alkaline-assisted stannation (MFI-AT1Sn005C). The parameter α reflects the advantage of using a hierarchical with respect to a purely microporous Sn-containing material in the isomerisation of the three sugars. The Stokes diameter is the effective diameter of the substrates in water as determined in previous studies (Qi *et al.*, *Bioresour. Technol.*, 2011, **102**, 7111; Shaffer *et al.*, *Adv. Powder. Technol.*, 2011, **22**, 454).

$$\alpha = \frac{\text{Yield of isomer at } t = 15 \text{ min over the post-synthesis treated sample}}{\text{Yield of isomer at equilibrium over the post-synthesis treated sample}} - \frac{\text{Yield of isomer at } t = 15 \text{ min over Sn-MFI-P}}{\text{Yield of isomer at equilibrium over Sn-MFI-P}}$$

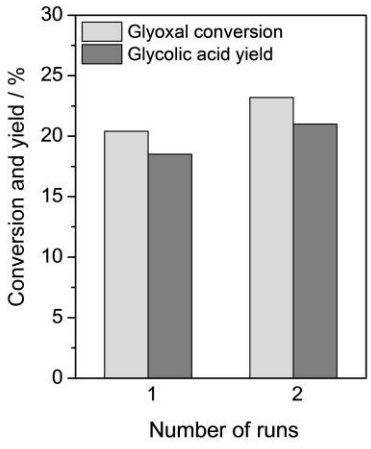

Fig. SI2. Conversion of glyoxal and yield of glycolic acid over MFI-AT1Sn005C at 363 K and 24 h in two consecutive catalytic runs.

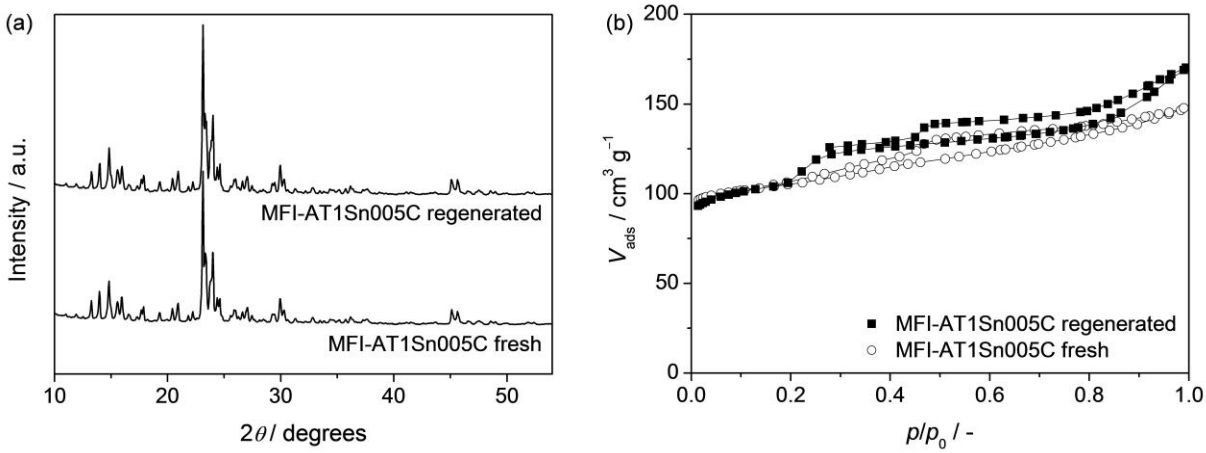

Fig. SI3. (a) X-ray diffraction patterns and (b) N_2 isotherms of MFI-AT1Sn005C in fresh form and after regeneration through calcination (823 K, 5 K min^{-1}, 5 h) in flowing air.

Table SI1 Yield of isomers (xylulose, fructose, and lactulose) over selected catalysts.

Substrate	Catalyst	Isomer yield at t =15 min	Isomer yield at t = 2 h
Xylose	Sn-MFI-AT1	6.5	8.5
	MFI-AT1Sn005C	6.9	8.2
Glucose	Sn-MFI-AT1	9.5	23.2
	MFI-AT1Sn005C	13.1	23.8
Lactose	Sn-MFI-AT1	12.1	22.5
	MFI-AT1Sn005C	17.0	24.5